

CHAPTER 111

WAVE RUNUP ON VERTICAL CYLINDERS

by

C. J. Galvin¹ and R. J. Hallermeier²

ABSTRACT

Wave height at a point on vertical cylinders is measured as a function of the orientation angle, α , between the normal from the point on the cylinder and the direction of travel of a single periodic train of waves. The wave height distribution, $H(\alpha)$, has a broad maximum around $\alpha = 0^\circ$ (facing into the waves) and a more restricted maximum at $\alpha = 180^\circ$. The maximum at $\alpha = 0^\circ$ increases with wave height in all cases, and the super-elevation has about the magnitude of the velocity head in the wave crest. In 21 different $H(\alpha)$ for which it is possible to determine the axis of symmetry by a simple objective test, 14 $H(\alpha)$ have axes of symmetry within $\pm 3^\circ$ of the direction of wave travel. Most of the variation in $H(\alpha)$ is due to variation in crest elevation; trough elevation remains relatively constant for the 360° range of α . The shape of $H(\alpha)$ depends more on height and cylinder cross section than on period, although the variation in $H(\alpha)$ as a function of cross section is significantly less than the extreme variations in tested cross sections. Applications of these results to wave direction measurement and to interpretation of wave records from surface-piercing wave gages are discussed.

INTRODUCTION

As a wave passes a vertical cylinder, its shape, including its height, is affected by the presence of the cylinder. The purpose of this paper is to present measurements of wave height very near the surface of cylinders of selected cross sections. These experiments are motivated by the possibility that the wave height distribution around a cylinder can be used to measure wave direction. The height data in this paper are for periodic laboratory water waves propagating in one direction.

When a wave passes a vertical cylinder, the principal effects of the resulting wave-cylinder interaction are scattering by the cylinder and viscous dissipation in the wake of the cylinder (Chen and Mei, 1971). The parameter, $\pi X/L$, where X is the nominal cylinder diameter and L is the wavelength, describes the wave scattering, and the parameter, H/X , where H is the incident wave height, describes the wake effects. There should be a critical value of each parameter above which respective effects are significant, but these critical values are not known. Bidde (1970) suggests that eddy shedding by waves around a cylinder depends on a Keulegan-Carpenter number, $K = UT/X$, where U is the maximum fluid velocity and T is the wave period. In Bidde's (1970) experiments, eddy shedding occurs when $K > 3$.

¹Chief, Coastal Processes Branch, U. S. Army Coastal Engineering Research Center, Washington, D. C.

²Oceanographer, Coastal Processes Branch, U. S. Army Coastal Engineering Research Center, Washington, D. C.

The three dimensionless numbers, $\pi X/L$, H/X , and K , are collectively referred to in this paper as wave interaction parameters.

Only two previous experimental studies of wave height distribution around vertical cylinders are known to the authors (Hellström and Rundgren, 1954; Laird, 1955), and both of these studies are for a limited range of wave interaction parameters (Table 1). These early studies verify even casual observations that the wave height distribution around vertical cylinders is approximately symmetric about an axis given by the direction of wave travel.

TABLE 1. WAVE INTERACTION PARAMETERS* IN EXPERIMENTAL STUDIES OF WAVE HEIGHT AT CYLINDERS

		(1) $\pi X/L$	(2) H/X	(3) UT/X
This paper	Circular cylinders and H-beams	0.015 to 0.15	0.25 to 4.0	2 to 15
Hellström and Rundgren, 1954	Cylindrical model lighthouse	~ 1.0	~ 0.4	
Laird, 1955	Cylindrical model island	~ 1.0	~ 0.05	

*Column (1) is the scattering parameter; column (2) is the wake parameter; column (3) is the Keulegan-Carpenter number for eddy shedding (Bidde, 1970). X is diameter of cylinder, H is wave height, T is wave period. Both L (wavelength) and U (maximum particle velocity) are computed from linear theory.

TEST VARIABLES

Data were collected in CERC wave tanks 96 feet long by 1.5 feet wide, and 85 feet long by 14 feet wide. Each tank has a piston-type wave generator consisting of a vertical flat plate constrained to move horizontally in approximately simple harmonic motion, so that the generator motion is uniquely determined (in theory) by the period, T , and eccentric, E , of the driving arm (Galvin, 1964). In practice, the generator in the 85-foot tank vibrates badly, introducing higher frequency bumps in the wave record, especially for low waves.

The downstream end of the tanks have absorbing beaches designed to minimize reflection, and reflection was not considered a problem in these tests.

The wave height distribution around the cylinder depends on three sets of independent variables:

$$\text{Height Distribution} = f(H, \text{Cylinder, Gage}) \quad (1)$$

The first set, including 4 variables, determines the wave height, H , in the absence of the cylinder

$$H = H(T, E, d, x_g) \quad (2)$$

where d is the water depth and x_g is the distance from the generator to the cylinder. Distance, x_g , is required because the wave deforms nonlinearly as a function of distance traveled (Galvin, 1972).

The second set of independent variables describe the cylinder, including cylinder shape, size, and material. For the purpose of this paper, the term 'cylinder' includes any shape that can be formed by moving a vertical line around a closed curve. In this sense, the 7 shapes shown in Figure 1 are sections of cylinders. Cylinders A and B are circular cylinders; Cylinder C is the finned cylinder; Cylinders D, E, and F are the deep H-beam, the square H-beam, and the shallow H-beam, respectively; and Cylinder G is the flat plate. These cylinders vary in dimensions from a minimum of 0.5 inches for the thickness of the flat plate to a maximum of 12 inches for the diameter of the outer circumference of the finned cylinder. Cylinders A through F were made of Plexiglas: 1/8-inch thick for Cylinders A and E, and 1/4-inch thick for Cylinders B, C, D, and F. Cylinder G is varnished plywood. In addition to those shown on Figure 1, a number of other cylinders were tested for special purposes, including scale effects.

The third set of independent variables are the characteristics of the wave gage used to measure the height, including accuracy, distance between cylinder surface and gage, and position of the gage with respect to the cylinder cross-sectional shape. Accuracy and distance from the cylinder are discussed in the next section. The position of the gage on the cylinder for non-circular cylinders is always between flanges and as close as possible to the middle of the web surface (Figure 2).

The angle, α , to which the height distribution is referred, is the angle between the incoming wave direction and a line from the cylinder axis to the wave gage (Figure 2). The wave height distribution is then indicated by $H(\alpha)$, which was measured by rotating the cylinder-gage combination through 360° in 5 or 10-degree increments.

The range of conditions tested at each of the cylinders is shown on Table 2. The variables, H , T , and d were chosen to be Froude models of representative wave conditions at the CERC wave gage on the end of the Atlantic City, New Jersey, Steel Pier (1:15 for 96-ft tank; 1:6 for 85-ft tank). Because of test restrictions, including size of available wave gages, the cross sections of the laboratory cylinders are larger than required by the model scales, if existing piling and H-beams in the field are considered to be prototype (see Figure 1).

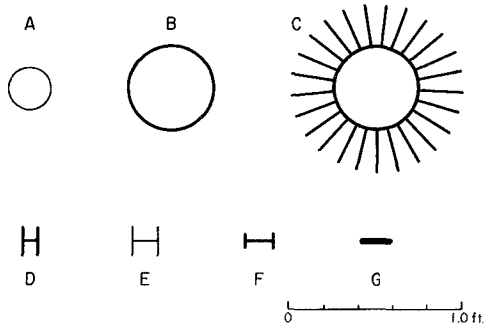


Figure 1. CROSS-SECTION OF TEST CYLINDERS

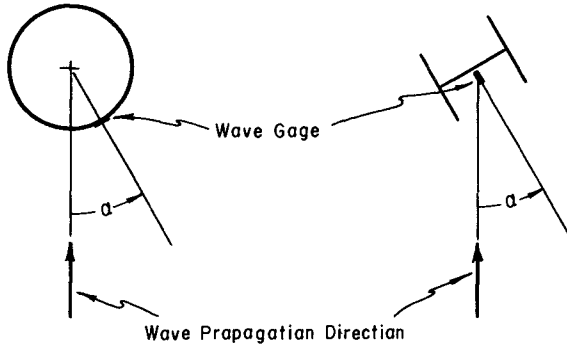
Figure 2. ORIENTATION ANGLE, α

TABLE 2. TEST CONDITIONS

Water Depth*, d, ft	Wave Period, T, sec	Wave Length**, L, ft	Wave Height, H, ft	Cylinders Tested
1.00	1.55	8.1	0.12-0.30	A,D,E,F,G
1.00	2.32	12.7	0.08-0.48	A,D,E,F,G
1.00	3.10	17.4	0.06-0.26	A,D,E,F,G
2.33	2.35	18.8	0.26-0.71	B,C,E
2.33	3.55	29.4	0.29-0.78	B,C,E
2.33	4.70	40.4	0.42-0.88	B,C

* x_g = 25.05 ft for 1.0 ft depth; 19.5 ft for 2.33 ft depth.

**Computed from linear theory for indicated depth and period.

WAVE HEIGHT ACCURACY

Three variations of the CERC parallel wire gage (Stafford, 1972) were used to measure $H(\alpha)$. Gages were checked for calibration and drift before and after each run, and in the case of the circular cylinders, some runs were checked independently by marking the height distribution with grease pencil (china marker) on the cylinder and by slipping a sheet of bond typing paper around the cylinder and letting the waves record their own crest height distribution in wetting the papers. These checks indicate that the data are internally consistent and usually repeatable to within a few percent. In one repeat test, a wetting agent (Edwal Kwik-Wet) was added to give the tank a 40 ppm solution of water with low surface tension. With this solution, the observed $H(\alpha)$ was not significantly different from $H(\alpha)$ without the solution, except over about 15% of the circle where the solution seemed to accentuate two minimums in $H(\alpha)$ by up to 20%. Changing the cylinder-to-gage distance by 3/4 to 1 inch changes wave height by 2 to 3% and crest height by 1 to 8%. These tests indicate that cylinder-to-gage distance does not significantly affect the conclusions of this study.

RESULTS

Experimental results presented here include information on wave shape (Figures 3, 4, 5, 6), symmetry of height distribution (Figure 7), effect of period on height distribution (Figure 8), and effects of height and cylinder cross section on the height distribution (Figures 9, 10, 11, 12, 13, 14).

Wave Shape. Experience shows that it is useful to define the height, H , as the sum of a crest height, P , and trough height, Q , as shown on Figure 3

$$H = P + Q \quad (3)$$

In terms of height distributions, the height at orientation angle α is

$$H(\alpha) = P(\alpha) + Q(\alpha) \quad (4)$$

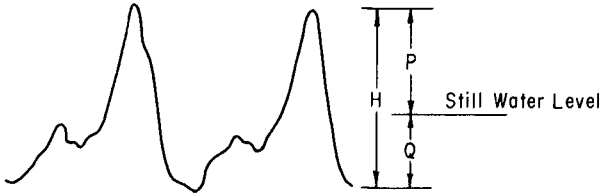


Figure 3. WAVE HEIGHT DEFINITIONS

Experiments show that most of the variation in $H(\alpha)$ is due to variation in $P(\alpha)$ (Figure 4), so that variations in $H(\alpha)$, which are the primary interest of this study, are also illustrated by variations in $P(\alpha)$. Since this crest height distribution, $P(\alpha)$, is easier to reduce from wave records than $H(\alpha)$, the remainder of the paper contains data in terms of $P(\alpha)$, unless otherwise stated. For easier comparison of results, the observed $P(\alpha)$ is divided by P , the crest height in the absence of the cylinder, in Figures 8 through 14.

The shape of the wave measured at the surface of the cylinder depends on the nonlinear deformation of the wave during its travel from the generator to the cylinder, and on the interaction between the cylinder and the wave. For d/L ratios less than about 0.1, individual water waves separate into 2 or more waves (solitons) of unequal height whose speeds are related to their respective heights (Galvin, 1972). Because their speeds differ, the separation between two solitons is a function of x_g , the distance from the generator. Thus, on Figure 5, the separation is greater between solitons than on Figure 6 because the dimensionless travel, x_g/L , is 1.97 for Figure 5, compared to 0.66 for Figure 6. Soliton separation does affect the shape, but not the basic symmetry of $H(\alpha)$. Only two values of x_g were used for data reported here (Table 2).

Figure 5 shows the effect of the wave-cylinder interaction due to:

- (1) wave steepness (compare low steepness shapes in left column with high

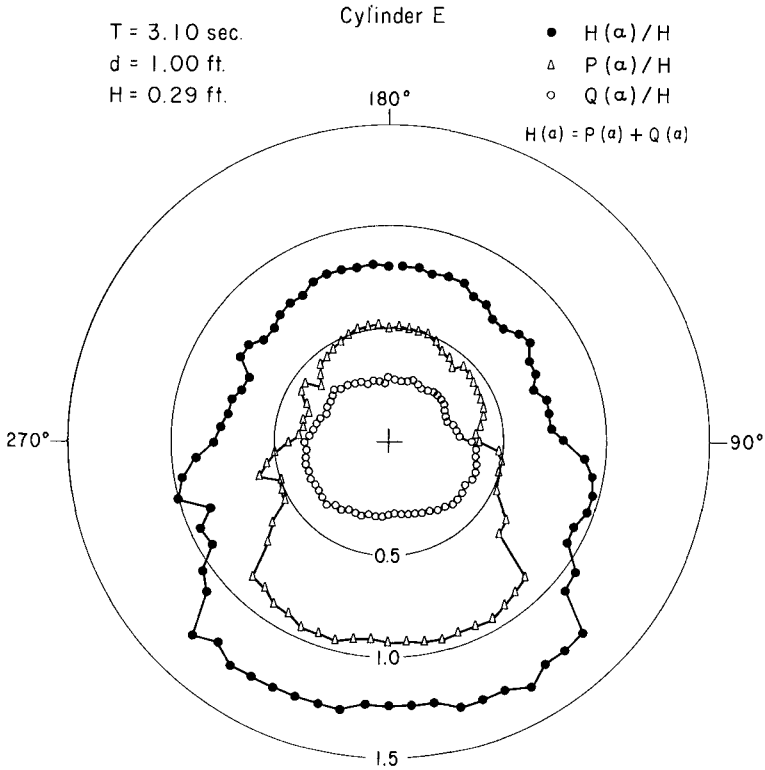


Figure 4. SIMILARITY BETWEEN $H(\alpha)$ AND $P(\alpha)$ IN SQUARE H-BEAM

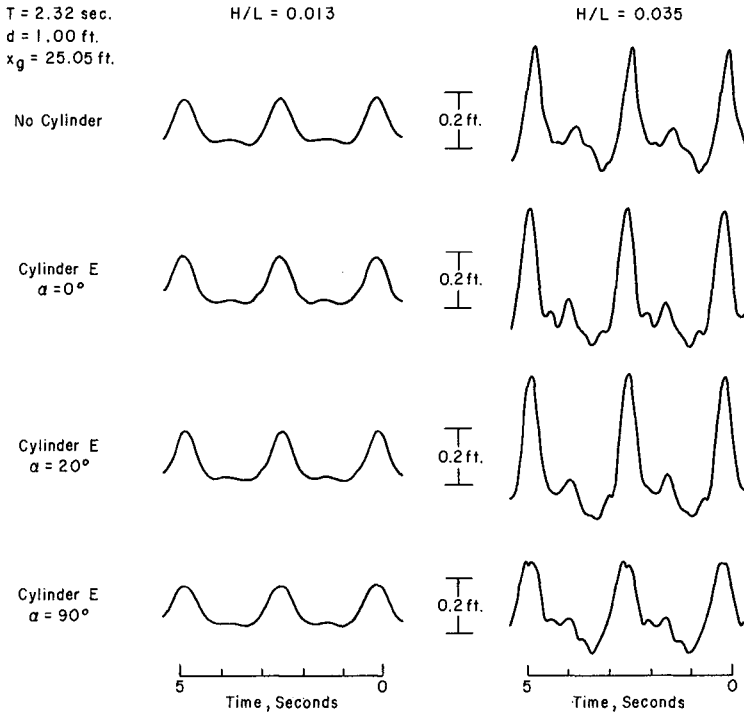


Figure 5. WAVE SHAPE IN SQUARE H-BEAM FOR TWO STEEPNESSES AND THREE ORIENTATIONS

$T = 3.55 \text{ sec.}$, $d = 2.33 \text{ ft.}$, $H/L = 0.029$, $x_g = 19.5 \text{ ft.}$

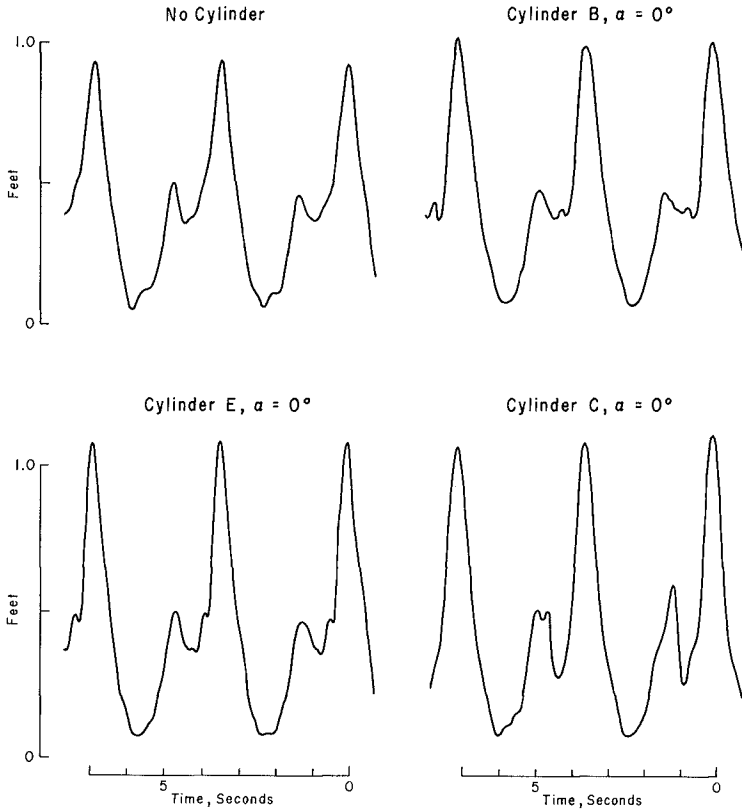


Figure 6. WAVE SHAPE AT THREE CYLINDERS FOR $\alpha = 0^\circ$

steepness shapes in right column); (2) presence of H-beam (compare top wave shapes without the H-beam to the remaining shapes with the H-beam); and (3) orientation angle ($\alpha = 0^\circ, 20^\circ, 90^\circ$). At low steepness, wave shape is not affected much either by the presence of the H-beam or by orientation. At high steepness, the cylinder and α alter both the crest elevation and the higher frequency oscillations in the trough. Among other phenomena, the steep wave at $\alpha = 20^\circ$ for these test conditions is repeatably smoother than the same wave with no H-beam (Figure 5).

Figure 6 shows wave shapes at three very different cylinders (circular cylinder, finned cylinder, square H-beam). Each of the cylinders amplifies the crest elevation compared to the elevation in the absence of the cylinder, but the shape of the wave does not differ much among cylinders. The amplification of the smaller soliton peak at the finned cylinder (lower right of Figure 6) appears to be due to a resonance excited by the subsiding crest of the larger soliton in the slot between fins.

Symmetry. On Figure 4, the $H(\alpha)$ and $P(\alpha)$ have obvious symmetry about the direction of wave travel. For simple symmetric distribution of $H(\alpha)$, the difference between $H(\alpha)$ and $H(\alpha + 180^\circ)$ is necessarily zero at right angles to the axis of symmetry. (This result holds for symmetric distributions whose maxima occur on the axis of symmetry. It does not necessarily hold, even though the distribution is symmetric, if pronounced maxima or minima occur off the axis of symmetry, e.g., rectangular distributions on a polar plot.)

Figure 7 shows a typical plot of the 180° differences for both $H(\alpha)$ and $P(\alpha)$. The zero crossing is 2 or 3° from the 90° position required by symmetry. A total of 26 separate $P(\alpha)$ distributions are illustrated on the Figures of this paper. Of these, 21 have the simple distributions that require zero crossing at $\alpha = 90^\circ$ if symmetric. Of these 21, the zero crossings of 14 are within $\pm 3^\circ$, and 17 are within $\pm 5^\circ$, of $\alpha = 90^\circ$. The exceptions in the 26 cases are the deep H-beam, which gives a rectangular distribution, and very low waves, where the 180° difference becomes about equal to the expectable error in measured $P(\alpha)$.

Period Effect. Figure 8 shows the $P(\alpha)/P$ distribution for 3 test conditions in which period varied but depth and height were held constant. These data show that the shape is approximately independent of period, although the amplification of height around $\alpha = 0^\circ$ is 15% greater for the steepest wave. Because period has relatively little effect on the height distribution, the remainder of this paper concerns tests run at a single period, $T = 2.32$ seconds in 1.0 ft depth, or its Froude-related value of 3.55 seconds in 2.33 ft depth (Table 2). Since the Keulegan-Carpenter number is greater than 3 in most of these tests, variation in T only affects the scattering parameter (Table 1). Since there is little variation of shape of $P(\alpha)$ with T , it appears that the wave height distributions are relatively independent of scattering effects in these tests.

Crest Height Distribution. Figures 9 through 13 show the effect of varying wave height, at $T = 2.32$ seconds and $d = 1.0$ ft, on the 3-inch circular cylinder (Figure 9), deep H-beam (Figure 10), square H-beam (Figure 11),

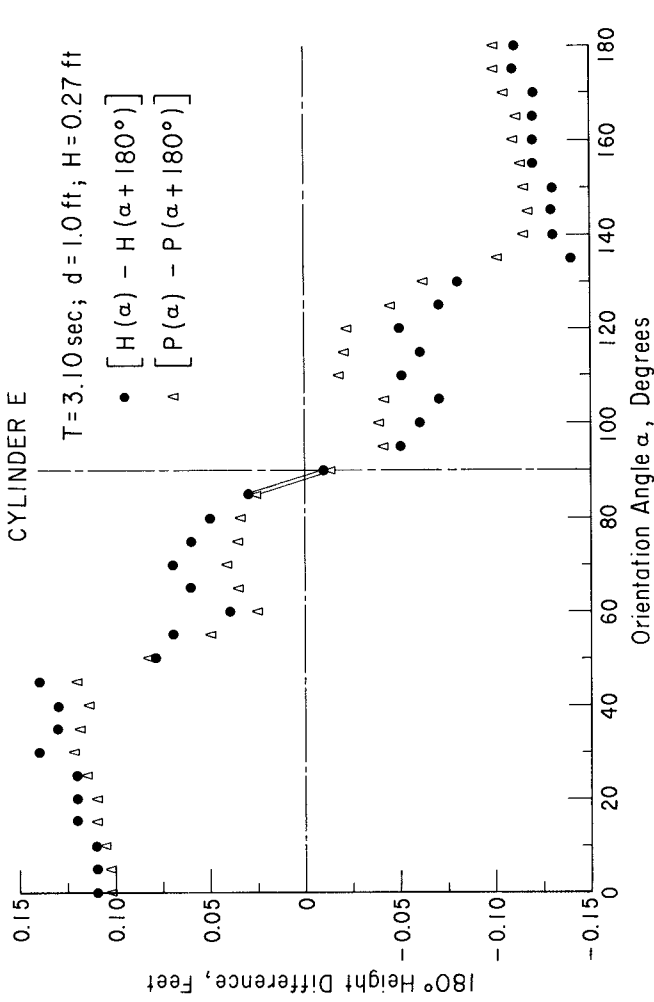


Figure 7. DEPENDENCE OF $[H(\alpha) - H(\alpha + 180^\circ)]$ AND $[P(\alpha) - P(\alpha + 180^\circ)]$ ON ORIENTATION ANGLE α (SQUARE H-BEAM)

Cylinder A, 3-inch Circular
H = 0.34 ft. (all tests)

- T = 1.55 sec., P = 0.167 ft.
- T = 2.32 sec., P = 0.223 ft.
- △ T = 3.10 sec., P = 0.256 ft.

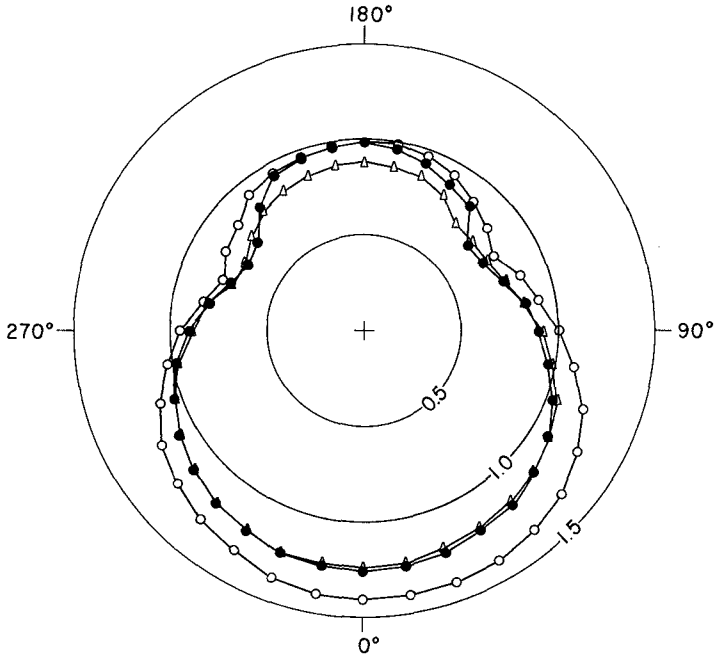


Figure 8. PERIOD EFFECT ON CREST HEIGHT DISTRIBUTION,
 $P(\alpha)/P$, FOR 3 PERIODS AT CONSTANT HEIGHT

shallow H-beam (Figure 12), and flat plate (Figure 13). Figure 14 (the last figure) compares the $P(\alpha)/P$ for 6-inch circular and finned cylinders. Figures 9 through 13 all have the same format, displaying $P(\alpha)/P$ for four test heights on three polar plots. The distribution for the lowest test height is repeated on each of the three polar plots as a reference distribution from which relative changes may be more easily judged.

For all distributions on Figures 9 through 13, the maximum value of $P(\alpha)/P$ occurs near $\alpha = 0^\circ$, or symmetrically about $\alpha = 0^\circ$. This front maximum has a magnitude that increases from about 1.0 to about 1.4 as P increases. On Figure 8, the maximum increases as T decreases. These facts are consistent with the hypothesis that runup on the front of the gage is the velocity head of the water particle in the wave crest. Use of linear or solitary wave theory to predict this runup gives results that are within a factor of 2 of observed values.

For almost all height distributions shown, there is also a pronounced maximum at $\alpha = 180^\circ$ (see Figure 12), but the value of this 180° maximum is not simply related to the wave height. This maximum in the rear is mainly stagnation head of converging flow in the rear of the cylinder as the crest passes, and it typically has a value between 0.8 and 1.0.

The existence of maxima at $\alpha = 0^\circ$ and $\alpha = 180^\circ$ requires minima at intermediate angles. These minima are observed to be related to separation points on the circular cylinder. From the data available, it appears that the minima on the equidimensional cylinders (circular cylinders and square H-beam) shift toward 180° as P increases (see Figures 9 and 11).

As a general test result, the shape of $P(\alpha)/P$ does not vary as much as the shape of the cylinder cross section. It appears that stagnation in the front of the cylinder and separation in the rear reduce the effect of cylinder shape on the flow.

ENGINEERING APPLICATIONS

Wave Direction Measurement. The symmetry in the $P(\alpha)/P$ distributions about the direction of travel suggests that the wave runup around a cylinder might be used to measure wave direction. Proposed wave direction instruments reported in the literature include: wave gage arrays, airborne cameras (Stilwell, 1969), radar (Oodshorn, 1960), acoustic (Multer, 1970) and electromagnetic sensors; devices to measure forces on small objects (Banwell, 1965), and vanes to align with or against the flow (Hall, 1950). Of the instruments suggested, wave gage arrays appear to have attracted the most attention (Barber, 1954, p. 1048; Panicker and Borgman, 1970, p. 117; Ploeg, 1972, p. 331; Chakrabarti and Snider, 1972, p. 657; Wiegel, Al-kazily, and Raïssi, 1972), but techniques of processing and interpreting the data are still under development. Except possibly for aerial photography, none of the proposed methods (including the method proposed here) have satisfactorily solved the problem of distinguishing directions when more than one wave train occurs at the same time. At present, no instrument is accepted as providing an economic, automatic field measurement of nearshore wave direction that is reliable to within 5 degrees. Due to refraction, at least 5 degree accuracy is needed for waves near the littoral zone. Considerable experience at the Coastal Engineering Research Center (Galvin and Seelig, 1971) and elsewhere (Zwamborn, et al, 1972) suggests that the best existing engineering solution to the problem of obtaining nearshore wave direction is visual observation.

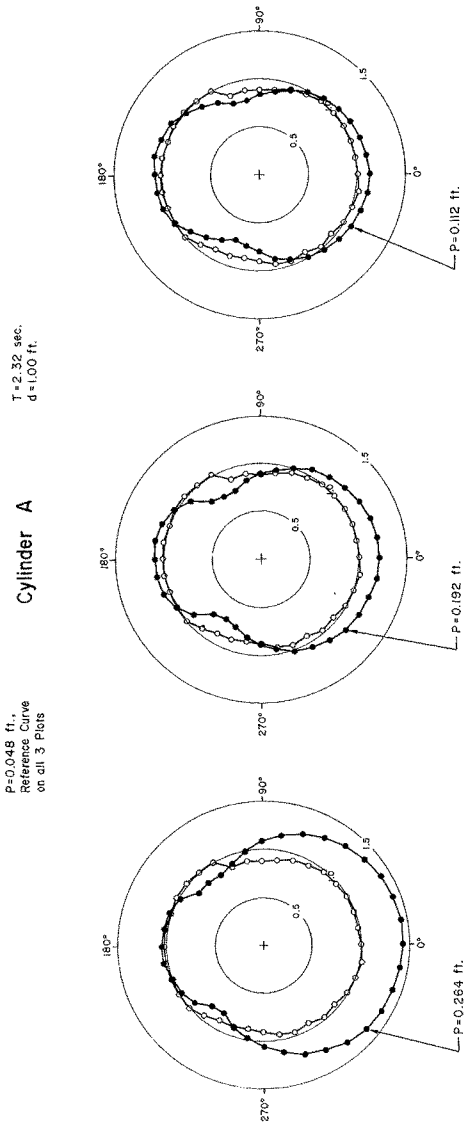


Figure 9. CREST HEIGHT DISTRIBUTION, $P(\alpha)/P$, FOR 4 HEIGHTS, CIRCULAR CYLINDER

° $P = 0.045$ ft.
 Reference Curve
 on all 3 Plots

Cylinder D

$T = 2.32$ sec.
 $d = 1.00$ ft.

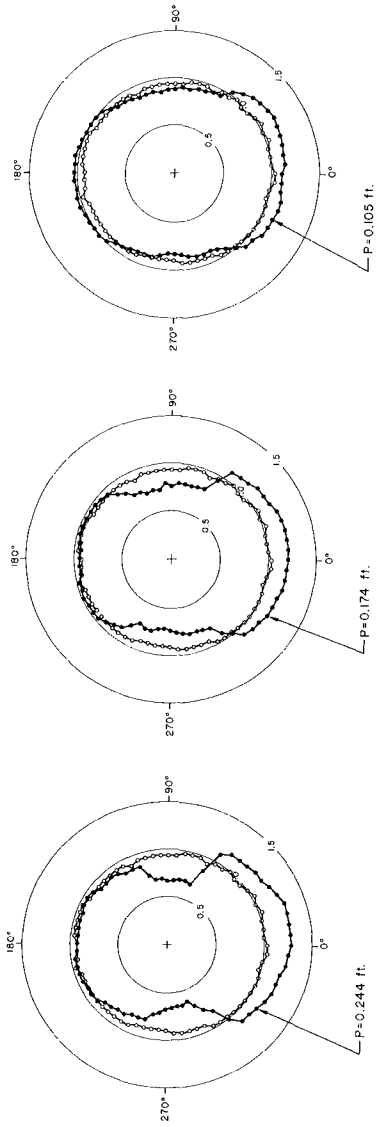


Figure 10. CREST HEIGHT DISTRIBUTIONS, $P(\alpha)/P$, FOR 4 HEIGHTS, DEEP H-BEAM

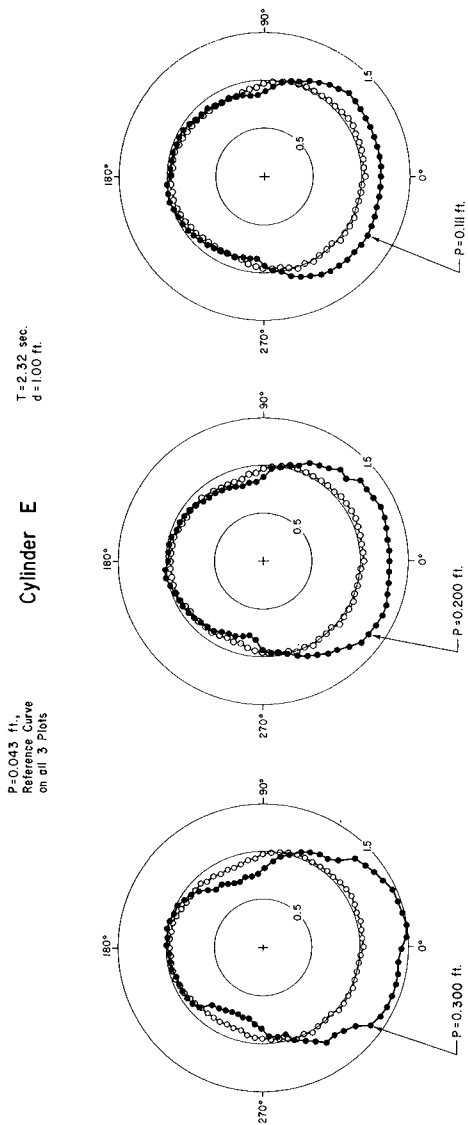


Figure II. CREST HEIGHT DISTRIBUTIONS, $P(\omega)/P$, FOR 4 HEIGHTS, SQUARE H-BEAM

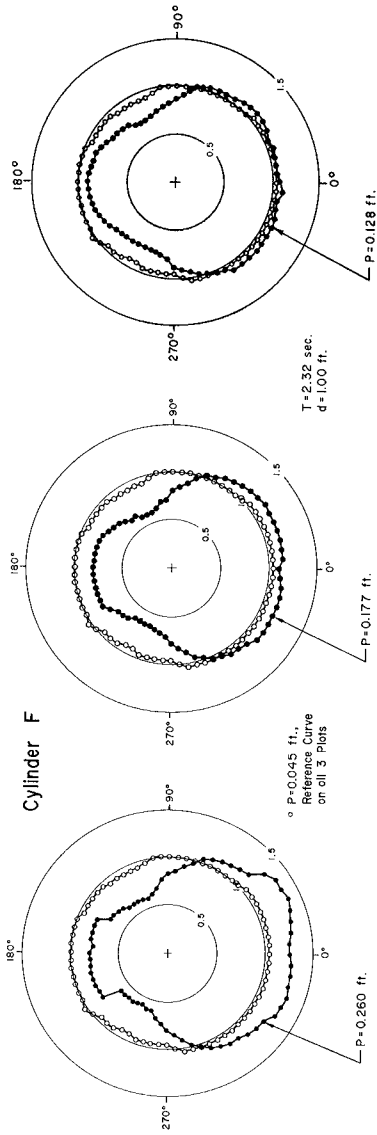


FIGURE 12. CREST HEIGHT DISTRIBUTIONS, $P(a)/R$, FOR 4 HEIGHTS, SHALLOW H-BEAM

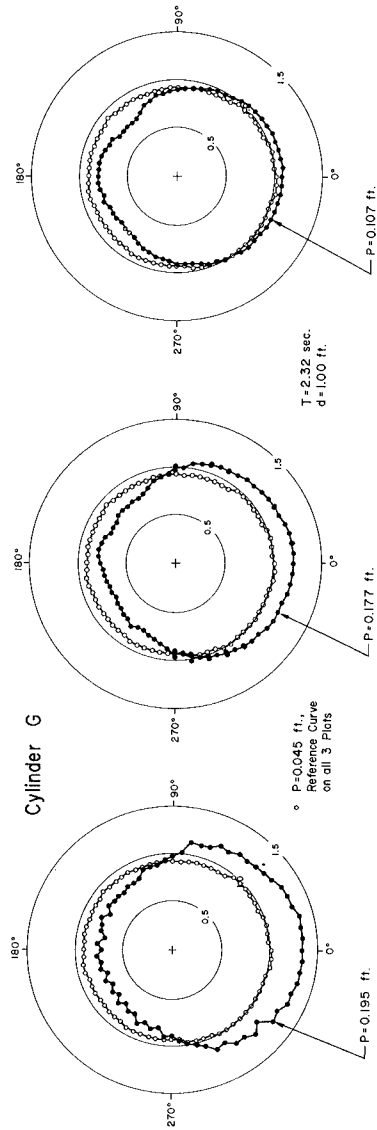


Figure 13. CREST HEIGHT DISTRIBUTIONS, $P(a)/R$, FOR 4 HEIGHTS, FLAT PLATE

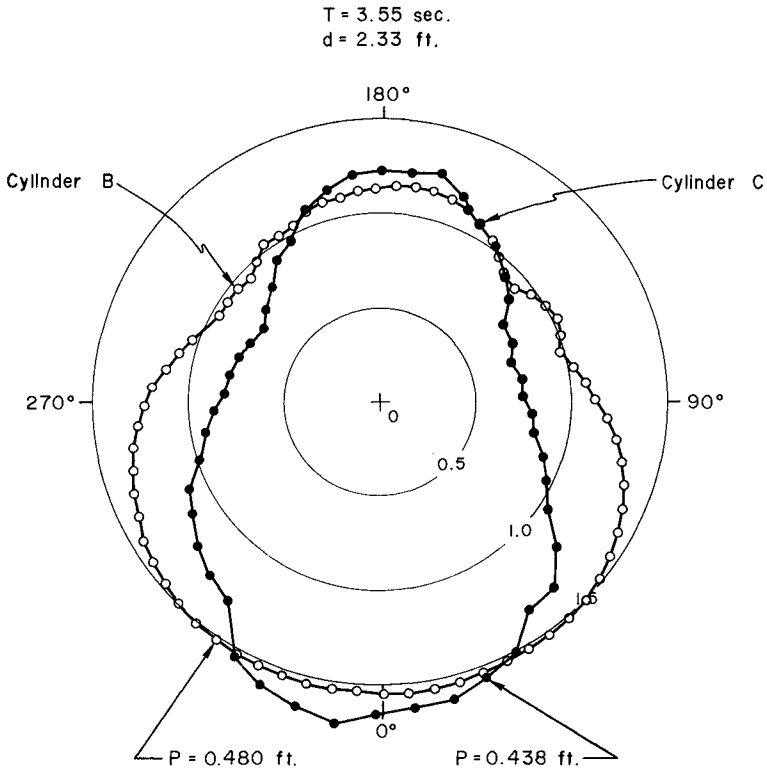


Figure 14. CREST HEIGHT DISTRIBUTIONS, $P(\alpha)/P$, FOR SIMILAR HEIGHTS, AT FINNED (•) AND 6-INCH (◦) CYLINDERS

The experiments of this paper suggest the use of wave gages mounted around a vertical cylinder as an instrument to measure wave direction. Advantages of this proposed method, that are not simultaneously present in other proposed methods, include: (1) effectively point measurement; (2) use of existing, field-proven sensors (wave gages or pressure sensors); (3) no moving parts; (4) performance that improves rather than degrades due to eddy-shedding and other viscous effects. The authors are unaware of published work on such an application, but field pressure records from around instrumented towers are now being analyzed for direction at the University of Florida with promising initial results (R. G. Dean, 1972, personal communication). A number of difficulties are anticipated in applying the proposed method, including the previously mentioned multiple wave train problem, as well as reduced sensitivity to low or short-crested waves, and design problems in developing a reliable field instrument.

Wave Gage Interpretation. Data from this study might be used to interpret wave height statistics obtained from surface-piercing wave gages mounted on structures. The step resistance wave gage that has been used for many years by the Coastal Engineering Research Center is typically mounted in an H-beam which is attached to a pier pile. These gages show heights that are higher than heights measured at the same point by wire surface-piercing gages or by submerged pressure gages (see Esteva and Harris, 1970, Figure 5). The difference increases with increasing height, which is consistent with wave runup on the gage as the cause, since velocity head in the wave crest is proportional to the square of the wave height. If real, these runup effects on wave gages overrepresent the high waves at a locality, and they could result in over conservative design. It was the field observation of runup effects on step resistance gages by one of the authors that led to the present study.

In addition to possible applications to wave direction measurement and to interpretation of some wave gage records, the data from this study have basic application to the problem of wave action on cylinders, a subject of continuing interest to coastal engineers.

ACKNOWLEDGEMENTS

The experiments and data reduction that form the basis of this paper were done between February 1970 and August 1972 by R. J. Karlitskie, C. R. Schweppe, R. E. L. Ray, and J. C. Jones at the U. S. Army Coastal Engineering Research Center. Data presented in this paper, unless otherwise noted, were obtained from research conducted by the United States Army Coastal Engineering Research Center under the Civil Works research and development program of the United States Army Corps of Engineers. Permission of the Chief of Engineers to publish this information is appreciated. The findings of this paper are not to be construed as official Department of the Army position unless so designated by other authorized documents. The contents of this paper are not to be used for advertising or promotional purposes. Citation of trade names does not constitute an official endorsement or approval of the use of such commercial products.

REFERENCES

- Banwell, T.J., "The TCB Wave Cage: A New Instrument for the Measurement of Ocean Waves", *Ocean Science and Engineering*, Vol. 2, pp. 1069-1087 (1965).
- Barber, N.F., "Finding the Direction of Travel of Sea Waves", *Nature*, Vol. 174, 1954, pp. 1048-1050.
- Bidde, D.D., "Wave Forces on a Circular Pile Due to Eddy Shedding", U. of California (Berkeley), Hydraulic Engineering Lab Report No. HEL 9-16, June, 1970.
- Chakrabati, S.K., and R.H. Snider, Laboratory simulation of multidirectional spectra of ocean waves, Offshore Technology Conference, Preprints, Volume II, paper OTC 1691, pp. 657-668, May 1972.
- Chen, H.S. and C.C. Mei, "Scattering and Radiation of Cravity Waves by an Elliptical Cylinder", MIT Parsons Laboratory Report No. 140, Aug 1971, 149 pp.
- Esteva, Dinorah, and D. Lee Harris, "Comparison of Pressure and Staff Cage Records", Proceedings of the 12th Conference on Coastal Engineering, ASCE, 1970, pp. 101-116.
- Galvin, C.J., "Finite-amplitude, Shallow-water Waves of Periodically Recurring Form, Proceedings of Symposium on Long Waves, Newark, Delaware, (in press), 1972.
- Calvin, C.J., "Wave-Height Prediction for Wave Generators in Shallow Water", CERC T.M. No. 4, 1964.
- Calvin, C.J., Seelig, W.N., "Nearshore Wave Direction from Visual Observations", EOS Abstract, AGU, Volume 52, No. 4, April 1971.
- Hall, Jay V., "The Rayleigh Disk as a Wave Direction Indicator", Beach Erosion Board, T.M. No. 18, July 1950.
- Hellstrom, B., and L. Rundgren, "Model Tests on Olands Sodra Grund Light-house", R. Inst. Tech. Stockholm, Bull. No. 39 of Inst. of Hydr., 1954, 64 pp.
- Laird, A.D.K., "A Model Study of Wave Action on a Cylindrical Island", *Trans American Geophysical Union*, 36, 1955, pp. 279-285.
- Multer, R.H., "Measuring a Directional Velocity in Water Waves with an Acoustic Flowmeter", USAE Coastal Engineering Research Center T.M. No. 31, (1970).
- Oudshoorn, H.M., "The Use of Radar in Hydrodynamic Surveying", Proceedings of the 7th Coastal Engineering Conference, The Hague, Netherlands, Vol. 1, pp. 59-76, (1960).
- Panicker, N.N., and L.E. Borgman, "Directional Spectra From Wave-Cage Arrays", 12th Coastal Engineering Conference, Washington, D.C., Sept. 1970, pp. 117-137, (ASCE).
- Ploeg, J., "Results of a Directional Wave Recording Station", Abstracts of 13th International Conference on Coastal Engineering, Vancouver, Canada, July 1972, pp. 331-337.
- Stafford, R.P., "Investigation and Procedure for Calibration of CERC Laboratory Wave Cage, FWK Model-1", CERC Laboratory Report (MFR), 27 July 1972.
- Stilwell, D., Jr., "Directional Energy Spectra of the Sea from Photographs", *Journal of Geophysical Research*, 74, pp. 1974-1986, (1969).
- Wiegel, R.L., M.F. Al-kazily, and Hooshang Raissi, "Wind Generated Wave Diffraction by a Breakwater, University of California Technical Report HEL 1-19, 130 pp., December 1971.
- Zwamborn, J.A., K.S. Russell and J. Nicholson, "Coastal Engineering Measurements", Thirteenth International Conference on Coastal Engineering Abstract